A multi-physics ensemble modeling framework for reliable C_n^2 estimation

Pierzyna, M.; Saathof, R.; Basu, S.

DOI
10.1117/12.2680997

Publication date
2023

Document Version
Final published version

Published in
Environmental Effects on Light Propagation and Adaptive Systems VI

Citation (APA)
Pierzyna, M., Saathof, R., & Basu, S. (2023). A multi-physics ensemble modeling framework for reliable C 2 n estimation. In K. Stein, & S. Gladysz (Eds.), *Environmental Effects on Light Propagation and Adaptive Systems VI* Article 127310N (Proceedings of SPIE - The International Society for Optical Engineering; Vol. 12731). https://doi.org/10.1117/12.2680997

A multi-physics ensemble modeling framework for reliable C2n estimation

Maximilian Pierzyna, Rudolf Saathof, Sukanta Basu

Maximilian Pierzyna, Rudolf Saathof, Sukanta Basu, "A multi-physics ensemble modeling framework for reliable C2n estimation," Proc. SPIE 12731, Environmental Effects on Light Propagation and Adaptive Systems VI, 127310N (19 October 2023); doi: 10.1117/12.2680997

SPIE.

Event: SPIE Remote Sensing, 2023, Amsterdam, Netherlands

A multi-physics ensemble modeling framework for reliable C_n^2 estimation

Maximilian Pierzyna[a], Rudolf Saathof[b], and Sukanta Basu[c]

[a]Department of Geoscience and Remote Sensing, Delft University of Technology, Delft, The Netherlands
[b]Faculty of Aerospace Engineering, Delft University of Technology, Delft, The Netherlands
[c]Atmospheric Sciences Research Center, University at Albany, Albany, USA

ABSTRACT

Free-space optical communication (FSOC) links are considered a key technology to support the increasing needs of our connected, data-heavy world, but they are prone to disturbance through atmospheric processes such as optical turbulence. Since turbulence is highly dependent on local topographic and meteorological conditions, modeling optical turbulence strength C_n^2 is challenging during the design phase of an optical link or network. Over the past 25 years, C_n^2 parameterizations of varying complexities have been combined with various numerical weather prediction models for the spatio-temporal estimation of C_n^2. However, the outputs of these models can exhibit substantial variability based on the user-defined configuration that determines how atmospheric processes are represented. To address this concern, we propose to run not a single model configuration but multiple diverse ones to generate an ensemble estimate of C_n^2. We employ the Weather Research and Forecasting model (WRF) with ten different planetary boundary layer (PBL) physics schemes forming a diverse ensemble yielding a probabilistic C_n^2 estimate. We demonstrate that this ensemble outperforms the individual runs when compared to scintillometer field measurements and show it to be robust against outliers. We believe that FSOC downstream tasks such as link budget estimations should also become more robust if based on a C_n^2 ensemble estimate compared to single model runs.

Keywords: Optical Turbulence, Free-Space Optical Communication, Mesoscale Modelling, Ensemble Modelling

1. INTRODUCTION

Free-space optical communication (FSOC) is considered a key technology to support the increasing needs of our connected data-heavy world by providing energy-efficient, secure links with high-data transmission capacity at potentially low cost. In contrast to traditional radio frequency communication, FSOC transmits data with an optical beam that propagates through the atmosphere. This propagating beam is disturbed by the atmosphere through, for example, clouds, particle/molecular scattering, and fluctuations of the atmospheric refractive index, the so-called optical turbulence.[1] Knowledge of these optical turbulence conditions is highly relevant for designing and deploying reliable, high-performance FSOC links, and there is an urge to quantify them well.[2] Turbulence strongly depends on the local topography and the ever-changing meteorological conditions. Hence, performance quantification of an FSOC link requires measuring or modeling the optical turbulence conditions for the time and site of (envisioned) operation. One modeling approach is to employ well-established mesoscale models to simulate the relevant atmospheric conditions of the link and estimate the optical turbulence strength C_n^2 in a post-processing step.[3,4] Mesoscale models, such as the Weather Research and Forecasting (WRF) model,[5] come with a multitude of physics schemes to parameterize different atmospheric processes of the atmosphere, such as radiation and turbulence. For each process, multiple options, i.e., multiple physics schemes, are offered that all aim to solve the same general problem but vary in underlying assumptions or simplifications and, consequently, in complexity and accuracy. As a result, the simulated meteorology can differ significantly between different model configurations. Notably, the choice of the Planetary Boundary Layer (PBL) scheme, which parameterizes

Send correspondence to M.P.: m.pierzyna@tudelft.nl

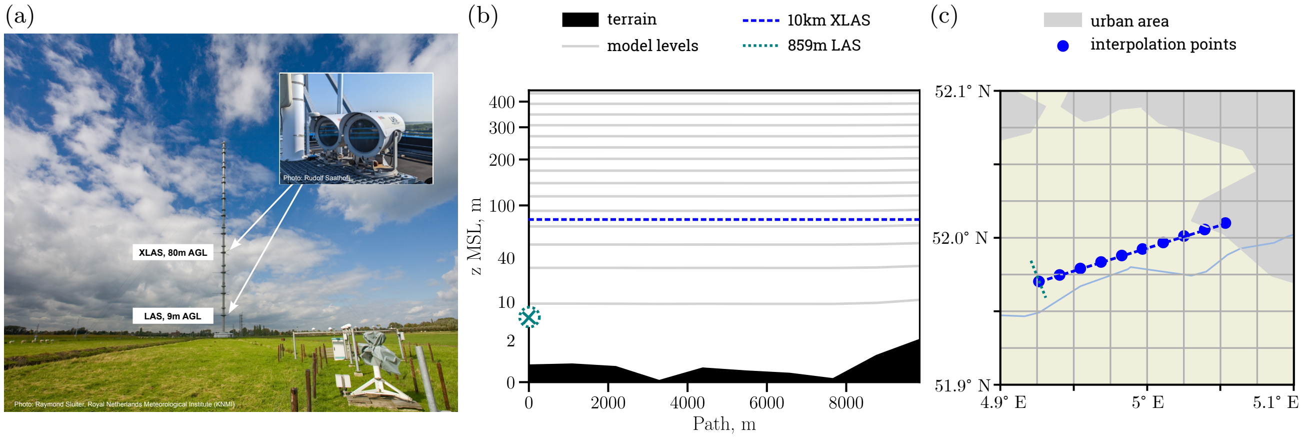

Figure 1: (a) Cabauw Experimental Site for Atmospheric Research (CESAR) with two scintillometers used to validate C_n^2 obtained from our probabilistic WRF simulation. The paths of both scintillometers are marked as dashed (blue) and dotted (green) lines in the sketches of (b) the vertical cross-section and (c) the top-down view of the CESAR site.

turbulent processes within the first ~ 1 km of the atmosphere, is expected to impact C_n^2 estimation significantly. At the same time, the PBL is the most relevant for FSOC because it distorts satellite uplinks and downlinks and is the region where terrestrial links operate.[1] However, the effect of different PBL schemes on C_n^2 estimation is challenging to assess a-priori. We propose to solve this issue by utilizing an ensemble of WRF models configured with different PBL schemes, similar to techniques successfully used for, e.g., precipitation forecasting.[6] Many PBL schemes have specific strong points, such as good performance of non-local schemes (e.g., the ACM2 scheme) in the daytime PBL, so a diverse PBL ensemble is expected to benefit from these specializations while being robust against outliers. Quantifying the ensemble spread yields information about the quality of the simulated C_n^2 and, subsequently, the expected quality of derived FSOC calculations, such as the link budget.

2. METHODOLOGY

To demonstrate the capability of our probabilistic C_n^2 simulation, we use the WRF model to simulate a 2-day test case with quiescent atmospheric conditions around the Cabauw Experimental Site for Atmospheric Research[7] (CESAR) in the Netherlands (cf. figure 1(a)). CESAR is selected because of the many instruments deployed, which serve for accuracy assessment of our WRF ensemble, and because it has been used as a test site for FSOC links.[8] Two scintillometers that measure C_n^2 along different paths are mounted at CESAR at different heights (see inset of figure 1(a)). Like FSOC links, scintillometers emit a laser beam at one end of the path and receive it at the other. C_n^2 is then derived by measuring the fluctuations in received power caused by optical turbulence along the path. At CESAR, a Large Apperture Scintillometer (LAS) is mounted at 9 m above ground, measuring along a 859 m path, and an EXtra Large Apperture Scintillomter (XLAS) operates at 80 m above ground along a 10 km path. Both scintillometer paths are marked in panels (b) and (c) of figure 1, which represent a vertical cross-section and a top-down view of the CESAR site, respectively.

The WRF ensemble is made up of ten individual WRF runs, so-called ensemble members, where each member is configured with a different PBL scheme. To connect the surface with the overlying atmosphere, WRF also requires configuring a surface layer (SL) scheme that depends on the selected PBL scheme, so we vary PBL and SL as PBL/SL pairs as listed in table 1. It is beyond the scope of this work to compare the schemes in detail, so the reader is referred to Skamarock et al.[5] for an overview or to the respective original publications of each scheme for in-depth discussions. Other physics options, such as microphysics or radiation schemes, are kept unchanged for all the simulations. In particular, we use WSM-5[9] for the microphysics, the Rapid Radiative Transfer Model for GCMs[10] (RRTMg) for long-wave and short-wave radiation, the Noah[11] land surface model, and the Modified Kain-Fritsch Scheme[12] to parameterize cumulus clouds in the largest domain. Each WRF simulation is forced with the same ERA5 reanalysis data provided by the European Centre for Medium-Range

Table 1: Planetary boundary layer (PBL) and surface layer (SL) schemes used for the 10 WRF models forming our ensemble. The numbers in the square brackets correspond to the WRF configuration option for `bl_pbl_physics` and `sf_sfclay_physics`.

	PBL scheme	SL scheme
●	Yonsei University (YSU)[13,14] [1]	Revised MM5 MO[15] [1]
■	Mellor-Yamada-Janjic (MYJ)[16,17] [2]	Eta MO similarity[17,18] [2]
⧫	QNSE with EDMF[19] [4]	QNSE[19] [4]
▼	Mellor-Yamada-Nakanishi-Niino (MYNN) 2.5[20,21] [5]	MYNN[22] [5]
▲	MYNN 3[20,21] [6]	MYNN[22] [5]
◀	Bougeault-Lacarrere (BouLac)[23] [8]	Eta MO similarity[17,18] [2]
▶	Grenier-Bretherton-McCaa (GBM)[24] [12]	Revised MM5 MO[15] [1]
★	TKE / TKE dissipation rate scheme (E-ϵ)[25,26] [16]	MYNN[22] [5]
✚	Asymmetrical Convective Model version 2 (ACM2)[27] [7]	Revised MM5 MO[15] [1]
⬢	University of Washington (UW)[28] [9]	MYNN[22] [5]

Weather Forecasts and set up with three nested domains with a final horizontal resolution of 1 km on the finest domain. The vertical resolution close to the surface ranges between 20 m and 30 m as can be seen in figure 1(b) depicting the model levels (grey lines).

Each run yields the temporal evolution of the 3D fields of mean potential temperature $\overline{\theta}$, mean wind components $(\overline{u}, \overline{v})$, relative humidity, and atmospheric pressure, from which we estimate C_n^2 following the gradient-based parametrization of Wyngaard et al. (1971, W71 hereafter).[29] W71 is selected because it only requires the aforementioned meteorological variables, readily available from any PBL scheme. However, W71 is only applicable in the lower 10% of the PBL, the surface layer (SL), which changes in depth throughout the day. Typically, the SL is shallow during the night ($\sim$10 m) and deep during the day ($\sim$100 m),[30] so the height until which W71 can be applied also changes. Therefore, our current approach cannot be used to estimate C_n^2 during the night for FSOC links or instruments mounted at large heights. Alternative C_n^2 parameterizations,[4,31] which are applicable anywhere in the PBL, depend on higher-order turbulence variables, such as turbulent kinetic energy, which not all PBL schemes yield. Selecting these parameterizations would limit the number of applicable PBL schemes and, thus, the ensemble diversity. Since in this study we target diversity, we accept the current surface layer constraint.

The agreement between probabilistic $\log_{10} C_n^2$ estimated from the WRF ensemble and the respective scintillometer observations is quantified on two levels: the individual member level and the ensemble level. To compare each individual model to the observations, the mean absolute error (MAE) and the Pearson correlation coefficient r are used. The MAE can be interpreted as a distance between simulated and observed time series, and the correlation coefficient quantifies how well the pattern of the time series (e.g., the diurnal cycle) is matched where $r = 0$ means no correlation and $r = 1$ perfect correlation. The Continuous Ranked Probability Score[32] (CRPS) is employed to compare the predicted $\log_{10} C_n^2$ distribution, i.e., the entire ensemble, against the observations. The CRPS can be considered as a probabilistic distance and is comparable to the MAE.[32]

3. RESULTS

The simulated probabilistic C_n^2 is compared to the observed scintillometer data in figure 2. Both time-series plots show that the median ensemble estimates of $\log_{10} C_n^2$ in panel (a) match observations from XLAS and LAS well in magnitude and the diurnal cycle. Note that no estimates are made for the XLAS during the night because the SL is expected to be shallower than the mounting height of the XLAS. The dark 50% uncertainty bands of the probabilistic simulations are relatively narrow, indicating consistency between the ensemble members. Only the 90% uncertainty band of the simulated C_n^2 time series at the XLAS location expands significantly during daytime. Responsible for the enhancement of uncertainty are two poorly performing members that are identified in panel (d) as BouLac/Eta (◀) and E-ϵ/MYNN (★) due to their considerable overestimation of

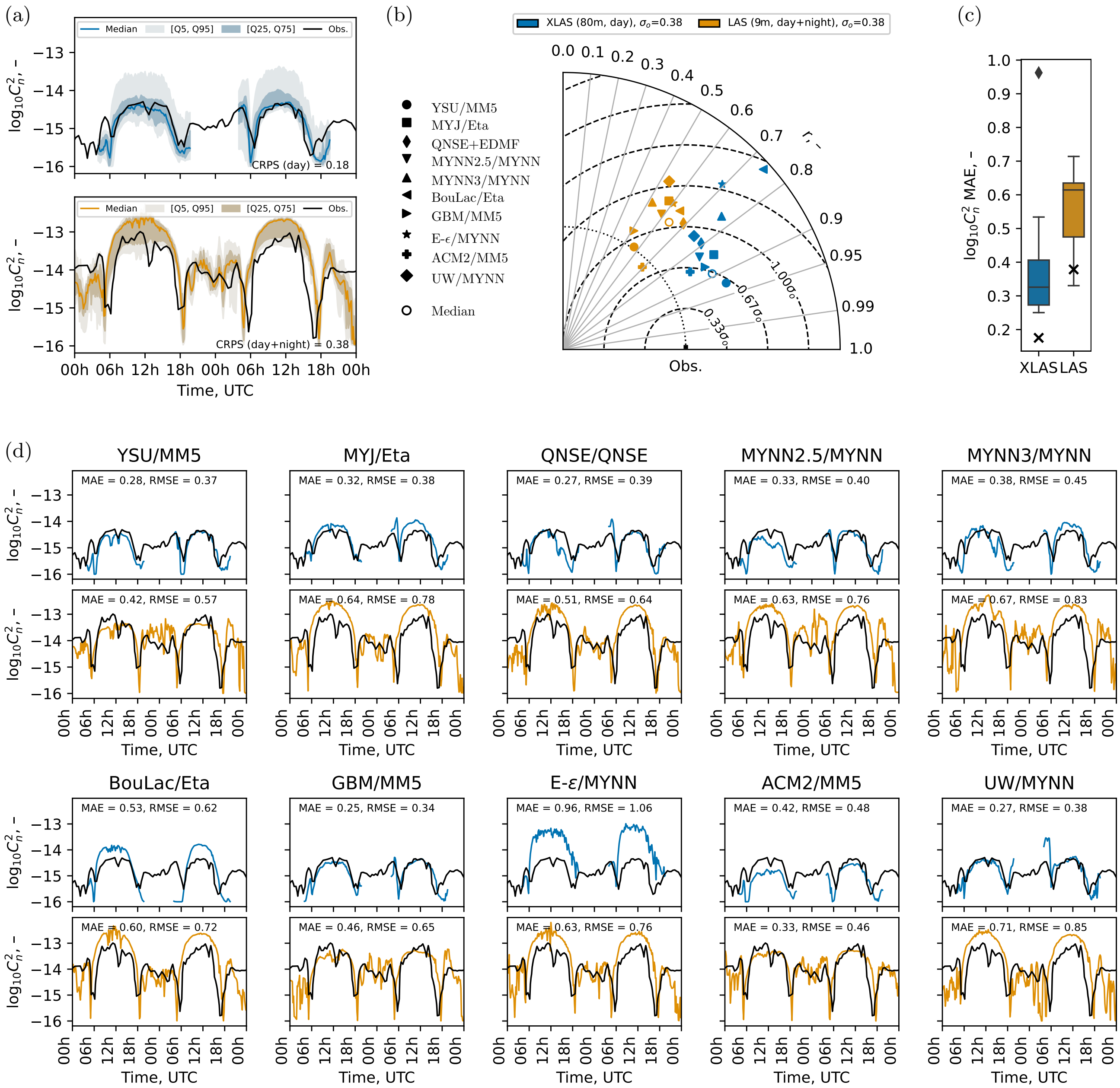

Figure 2: Comparison of $\log_{10} C_n^2$ estimates from the WRF simulations against scintillometer observations as (a) ensemble time series and (b) individual member model performance quantified by correlation (azimuthal) and relative error (concentric circles around observations). Distributions of members' MAE are compared to CRPS of the full ensemble in (c), and individual C_n^2 time series produced by each ensemble member are shown in (d). The titles in (d) correspond to the PBL/SL configurations listed in table 1. Night-time estimates for the XLAS location are excluded from the entire analysis because the surface layer is expected to be too shallow for W71 to be applicable.

the daytime C_n^2 values at the XLAS location. This exemplifies how some PBL schemes can perform poorly in one condition but well in others (e.g., for the C_n^2 values at the LAS location). The strength of the ensemble is its robustness against such conditionally low performance of a few members. BouLac/Eta and E-ϵ/MYNN are also visible as outliers in the Taylor diagram[33] in panel (b). The Taylor diagram shows the correlation coefficient r in azimuthal direction and increasing relative error as increasing distance between the configuration markers and the observation on the x-axis. Most of the markers are right of the dotted circle, indicating that most ensemble members overestimate $\log_{10} C_n^2$ on average, as visible also in the time series in (a). Except for the two outlier configurations, most ensemble members form a cluster around the median (○), showing inter-model agreement. The overall performance of the ensemble is compared to the individual performance of its members in panel (c). The two box plots present the distribution of the MAE computed between simulated $\log_{10} C_n^2$ and the observations for each model, and the black crosses represent the mean CRPS. Since CRPS and MAE are comparable metrics, the CRPS values lower than most MAE values demonstrate that the probabilistic C_n^2 estimate outperforms almost all the individual ones.

4. CONCLUSION

In summary, we demonstrated that our probabilistic C_n^2 WRF ensemble not only captures measurements in the surface layer but also outperforms almost all the individual deterministic model runs. We also showed the more general advantages of ensemble approaches, such as their robustness against outliers and the possibility of using the ensemble spread as a reliability measure. We believe these advantages to be also highly relevant in the FSOC context when FSOC calculations are based on a probabilistic simulation rather than a deterministic one. For example, in situations where validation data are not available – at new sites or for forecasts into the future –, we envisage that the ensemble's robustness and its uncertainty bands will make it more trustworthy than single runs. Also, downstream tasks, such as link budget calculations or link availability estimates, become potentially more reliable if they are based on robust C_n^2 estimates. The disadvantage of our methodology is increased computation time, which should be weighed with the advantages on a per-case basis. We also note that a more extensive study is needed that covers more than two days to support our results further. Future ensembles could also vary other physics options, such as the microphysics scheme, which is expected to be significant under precipitating conditions. To extend the applicability beyond the SL, more advanced C_n^2 parametrizations[4,31,34] can be used, but at the cost of a reduced ensemble diversity due to fewer applicable PBL schemes.

ACKNOWLEDGMENTS

This publication is part of the project *FREE – Optical Wireless Superhighways: Free photons (at home and in space)* of the research programme TTW-Perspectief, which is (partly) financed by the Dutch Research Council (NWO, project number P19-13). The scintillometer data used for validation were generated in the Ruisdael Observatory, a scientific research infrastructure, which is (partly) financed by the Dutch Research Council (NWO, grant number 184.034.015).

REFERENCES

[1] Jahid, A., Alsharif, M. H., and Hall, T. J., "A contemporary survey on free space optical communication: Potentials, technical challenges, recent advances and research direction," *Journal of Network and Computer Applications* **200**, 103311 (Apr. 2022).

[2] Kaushal, H. and Kaddoum, G., "Optical Communication in Space: Challenges and Mitigation Techniques," *IEEE Communications Surveys & Tutorials* **19**(1), 57–96 (2017).

[3] Bougeault, P., Hui, C. D., Fleury, B., and Laurent, J., "Investigation of seeing by means of an atmospheric mesoscale numerical simulation," *Applied Optics* **34**, 3481–3488 (June 1995).

[4] Masciadri, E., Vernin, J., and Bougeault, P., "3D mapping of optical turbulence using an atmospheric numerical model - I. A useful tool for the ground-based astronomy," *Astronomy and Astrophysics Supplement Series* **137**, 185–202 (May 1999).

[5] Skamarock, W. C., Klemp, J. B., Dudhia, J., Gill, D. O., Liu, Z., Berner, J., Wang, W., Powers, J. G., Duda, M. G., Barker, D. M., and Huang, X.-Y., "A Description of the Advanced Research WRF Model Version 4.3," tech. rep., UCAR/NCAR (July 2021).

[6] Vannitsem, S., Wilks, D., and Messner, J., eds., [*Statistical Postprocessing of Ensemble Forecasts*], Elsevier, Amsterdam, Netherlands (2019).

[7] Bosveld, F. C., Baas, P., Beljaars, A. C. M., Holtslag, A. A. M., De Arellano, J. V.-G., and Van De Wiel, B. J. H., "Fifty Years of Atmospheric Boundary-Layer Research at Cabauw Serving Weather, Air Quality and Climate," *Boundary-Layer Meteorology* **177**, 583–612 (Dec. 2020).

[8] Broekens, K., Klop, W., Moens, T., Eschen, M., do Amaral, G. C., Silverstri, F., Oosterwijk, A., Visser, M., Doelman, N., Kaffa, L., et al., "Adaptive optics pre-correction demonstrator for terabit optical communication," in [*International Conference on Space Optics—ICSO 2022*], **12777**, 758–766, SPIE (2023).

[9] Hong, S.-Y., Dudhia, J., and Chen, S.-H., "A Revised Approach to Ice Microphysical Processes for the Bulk Parameterization of Clouds and Precipitation," *Monthly Weather Review* **132**, 103–120 (Jan. 2004).

[10] Iacono, M. J., Delamere, J. S., Mlawer, E. J., Shephard, M. W., Clough, S. A., and Collins, W. D., "Radiative forcing by long-lived greenhouse gases: Calculations with the AER radiative transfer models," *Journal of Geophysical Research: Atmospheres* **113**(D13) (2008).

[11] Chen, F. and Dudhia, J., "Coupling an Advanced Land Surface–Hydrology Model with the Penn State–NCAR MM5 Modeling System. Part I: Model Implementation and Sensitivity," *Monthly Weather Review* **129**, 569–585 (Apr. 2001).

[12] Kain, J. S., "The Kain–Fritsch Convective Parameterization: An Update," *Journal of Applied Meteorology and Climatology* **43**, 170–181 (Jan. 2004).

[13] Hong, S.-Y. and Pan, H.-L., "Nonlocal Boundary Layer Vertical Diffusion in a Medium-Range Forecast Model," *Monthly Weather Review* **124**, 2322–2339 (Oct. 1996).

[14] Hong, S.-Y., Noh, Y., and Dudhia, J., "A New Vertical Diffusion Package with an Explicit Treatment of Entrainment Processes," *Monthly Weather Review* **134**, 2318–2341 (Sept. 2006).

[15] Jiménez, P. A., Dudhia, J., González-Rouco, J. F., Navarro, J., Montávez, J. P., and García-Bustamante, E., "A Revised Scheme for the WRF Surface Layer Formulation," *Monthly Weather Review* **140**, 898–918 (Mar. 2012).

[16] Mellor, G. L. and Yamada, T., "Development of a turbulence closure model for geophysical fluid problems," *Reviews of Geophysics* **20**(4), 851–875 (1982).

[17] Janić, Z. I., "Nonsingular implementation of the Mellor-Yamada level 2.5 scheme in the NCEP Meso model," Office Note 437, National Centers for Environmental Prediction (U.S.) (Jan. 2002).

[18] Janjic, Z. I., "The surface layer in the NCEP Eta Model," in [*Eleventh Conference on Numerical Weather Prediction*], 354–355, Amer. Meteor. Soc, Norfolk, VA (Aug. 1996).

[19] Sukoriansky, S., Galperin, B., and Perov, V., "'Application of a New Spectral Theory of Stably Stratified Turbulence to the Atmospheric Boundary Layer over Sea Ice'," *Boundary-Layer Meteorology* **117**, 231–257 (Nov. 2005).

[20] Nakanishi, M. and Niino, H., "An Improved Mellor–Yamada Level-3 Model: Its Numerical Stability and Application to a Regional Prediction of Advection Fog," *Boundary-Layer Meteorology* **119**, 397–407 (May 2006).

[21] Nakanishi, M. and Niino, H., "Development of an Improved Turbulence Closure Model for the Atmospheric Boundary Layer," *Journal of the Meteorological Society of Japan. Ser. II* **87**(5), 895–912 (2009).

[22] Dyer, A. J. and Hicks, B. B., "Flux-gradient relationships in the constant flux layer," *Quarterly Journal of the Royal Meteorological Society* **96**(410), 715–721 (1970).

[23] Bougeault, P. and Lacarrere, P., "Parameterization of Orography-Induced Turbulence in a Mesobeta–Scale Model," *Monthly Weather Review* **117**, 1872–1890 (Aug. 1989).

[24] Grenier, H. and Bretherton, C. S., "A Moist PBL Parameterization for Large-Scale Models and Its Application to Subtropical Cloud-Topped Marine Boundary Layers," *Monthly Weather Review* **129**, 357–377 (Mar. 2001).

[25] Langland, R. H. and Liou, C.-S., "Implementation of an E–ϵ Parameterization of Vertical Subgrid-Scale Mixing in a Regional Model," *Monthly Weather Review* **124**, 905–918 (May 1996).

[26] Zhang, C., Wang, Y., and Xue, M., "Evaluation of an E–ϵ and Three Other Boundary Layer Parameterization Schemes in the WRF Model over the Southeast Pacific and the Southern Great Plains," *Monthly Weather Review* **148**, 1121–1145 (Feb. 2020).

[27] Pleim, J. E., "A Combined Local and Nonlocal Closure Model for the Atmospheric Boundary Layer. Part I: Model Description and Testing," *Journal of Applied Meteorology and Climatology* **46**, 1383–1395 (Sept. 2007).

[28] Bretherton, C. S. and Park, S., "A New Moist Turbulence Parameterization in the Community Atmosphere Model," *Journal of Climate* **22**, 3422–3448 (June 2009).

[29] Wyngaard, J. C., Izumi, Y., and Collins, S. A., "Behavior of the Refractive-Index-Structure Parameter near the Ground*," *Journal of the Optical Society of America* **61**, 1646 (Dec. 1971).

[30] Stull, R. B., "An introduction to boundary layer meteorology," *Kluwer Academic Publishers* (1988).

[31] He, P. and Basu, S., "Mesoscale modeling of optical turbulence (C_n^2) utilizing a novel physically-based parameterization," in [*SPIE Optical Engineering + Applications*], van Eijk, A. M. J., Davis, C. C., and Hammel, S. M., eds., 96140K (Sept. 2015).

[32] Hersbach, H., "Decomposition of the Continuous Ranked Probability Score for Ensemble Prediction Systems," *Weather and Forecasting* **15**, 559–570 (Oct. 2000).

[33] Taylor, K. E., "Summarizing multiple aspects of model performance in a single diagram," *Journal of Geophysical Research: Atmospheres* **106**, 7183–7192 (Apr. 2001).

[34] Basu, S., Osborn, J., He, P., and DeMarco, A. W., "Mesoscale modelling of optical turbulence in the atmosphere: The need for ultrahigh vertical grid resolution," *Monthly Notices of the Royal Astronomical Society* **497**, 2302–2308 (Sept. 2020).